AD-A174 083 DIHYDRIDE TRANSFER A BIMOLECULAR MECHANISM IN THE ISOMERIZATION OF CIS-DI..(U) ROCHESTER UNIV NY DEPT OF CHEMISTRY A J KUNIN ET AL. 30 OCT 86 TR-13 1/1

UNCLASSIFIED N00014-83-K-0154 F/G 7/3 NL

END
DATE FILMED
1 87

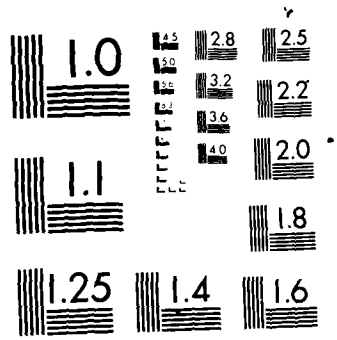

MICROCOPY RESOLUTION TEST CHART
NATIONAL BUREAU OF STANDARDS-1963-A

AD-A174 083

(12)

OFFICE OF NAVAL RESEARCH

Contract N00014-83-K-0154

Task No. NR 634-742

TECHNICAL REPORT NO. 13

Dihydride Transfer. A Bimolecular Mechanism in the Isomerization of cis-Dihydridobromo(carbonyl)(bis)(diphenylphosphino)ethane)iridium, $IrH_2Br(CO)(dppe)$

by

Amanda J. Kunin, Curtis E. Johnson, John A. Maguire,

William D. Jones* and Richard Eisenberg*

Prepared for Publication

in the

Journal of the American Chemical Society

University of Rochester

Department of Chemistry

Rochester, NY 14627

NOV 1 8 1986

A

October 30, 1986

DTIC FILE COPY

Reproduction in whole, or in part, is permitted for any purpose of the United States Government.

This document has been approved for public release and sale; its distribution is unlimited

86 11 14 070

Dihydride Transfer. A Bimolecular Mechanism in the Isomerization of cis-Dihydridobromotcarbonyl)(bis(diphenylphosphinoethane)iridium, $IrH_2Br(CO)(dppe)$

Amanda J. Kunin, Curtis E. Johnson, John A. Maguire,
William D. Jones* and Richard Eisenberg*
Department of Chemistry
University of Rochester
Rochester, New York 14627

Received

Abstract: The oxidative addition of H_2 to IrBr(CO)(dppe), 2, (dppe = 1,2-bis-(diphenylphosphino)ethane) yields a kinetic dihydride species, 3, which then isomerizes to a more stable isomer, 4. This isomerization of 3 to 4 has been studied kinetically as a function of initial H_2 pressure. Two pathways are operative at ambient temperature. The first is a reductive elimination/oxidative addition sequence which is first order in complex, while the second is a bimolecular pathway involving dihydride transfer from 3 to 2 to produce 4 and regenerate 2. The dihydride transfer pathway is second order in complex and becomes the dominant isomerization mechanism when less than one equivalent of H_2 relative to 2 has been added to the system. All of the kinetic data have been fit to a complete rate law which leads to a bimolecular rate constant for dihydride transfer of 0.21 M^{-1} min^{-1}. Below -20 °C, the dihydride transfer pathway for isomerization is the only one operating.

INTRODUCTION

The oxidative addition of H_2 to d^8 metal complexes has been extensively studied over the past 20 years because of its relevance to H_2 activation in homogeneous hydrogenation and hydroformylation.[1-2] One of the most thoroughly investigated systems in this context is Vaska's complex, trans-IrCl(CO)$(PPh_3)_2$ (1), which reacts with H_2 according to eqn (1).[3] Based on kinetic and mechanistic studies,[3-5] H_2 oxidative addition is generally viewed as a concerted process with a triangular MH_2 transition state leading to a cis dihydride product.

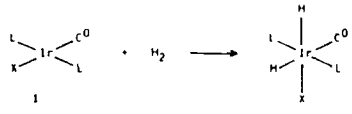

1 (1)

Recently we began investigating the oxidative addition chemistry of the related set of cis phosphine complexes IrX(CO)(dppe), 2, and have discovered that its concerted oxidative addition reactions proceed under kinetic control.[6,7] With complexes 2, the oxidative addition of H_2 can follow two possible pathways, i and ii, as shown in eqn (2), leading to different diastereomers, 3 and 4, respectively, for the concerted process. Pathway i corresponds to H_2 approach to the square planar complex with the molecular axis of H_2 parallel to P-Ir-CO as shown in A. The concerted oxidative addition along i takes place with a bending of the trans P-Ir-CO axis so that one hydride of the product becomes trans to CO and the other trans to P. Pathway ii corresponds to approach with the H_2 molecular axis parallel to P-Ir-X, as

QUALITY INSPECTED 4

A-1

shown in B, and addition occurs with bending of the P-Ir-X axis.

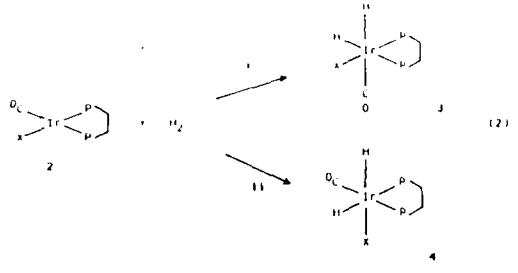

(2)

While two diastereomers thus exist for concerted H_2 oxidative addition to IrX(CO)(dppe), we have found that for X = Cl, Br, I, H, and CN, the initial oxidative addition takes place diastereoselectively along pathway I.[6] The reaction with H_2 in solution is essentially complete within 1 minute under an atmosphere of H_2, forming isomer 3 to >99%. That the reaction proceeds under kinetic control is illustrated by the fact that for X = Cl, Br, and I, the initially formed diastereomer slowly equilibrates with the more stable diastereomer corresponding to oxidative addition along pathway II. Based on the variation of X, a steric basis for the diastereoselectivity of H_2 oxidative addition was ruled out, leaving ligand electronic effects as the controlling factor in the diastereoselection process.

The isomerization of the kinetic isomer 3 to the thermodynamic isomer 4 for X = Br was also examined by us in detail.[6a] Based on the observation that 3 rapidly forms 3 d_2 when placed under D_2, it was determined that the initial oxidative addition is rapid and reversible, occurring much faster than isomerization. The isomerization in acetone under H_2 follows clean first order kinetics with an observed rate constant, k_{obs}, at 55 °C of 1.85×10^{-4} sec^{-1}, corresponding to a half-life of 62 minutes. At 25 °C the half-life of the kinetic isomer 3 is about 35 hours. Two possible mechanisms for isomerization appeared consistent with the kinetic data. The first was an intramolecular rearrangement while the second corresponded to a reductive elimination/-oxidative addition sequence with the formation of 2 as an intermediate. We favored this latter pathway, <u>ie.</u>, $3 \rightleftharpoons 2 + H_2 \rightarrow 4$, principally because reductive elimination of H_2 from 3 occurs much more rapidly than isomerization.

The clean first-order kinetics for the isomerization, however, were observed only in acetone solvent, and under an excess of hydrogen. When the reaction was studied in benzene, the isomerization proceeded much more rapidly with an apparent half-life of <u>ca.</u> 2 hours at 25 °C, although the kinetics were not found to be reproducible.[6a] The isomerization of 3 to 4 was also found to be inhibited by (TBA)Br and accelerated by added $AgBF_4$ in benzene and by added O_2 in acetone. Perhaps most puzzling was the observation that isomerization proceeded more rapidly in rigorously deoxygenated acetone when less H_2 was present. Since the proposed reductive elimination/oxidative addition sequence for isomerization possessed no kinetic dependance on H_2, our observation suggested that another mechanism for isomerization existed. We have therefore reinvestigated the isomerization of the kinetic isomer 3 to the thermodynamic isomer 4 as a function of H_2 pressure.

In this paper we describe in detail that investigation, including the observation that a second isomerization mechanism involving dihydride transfer between metal centers competes with the first order isomerization mechanism at

ambient temperature, and is the sole mechanism operating at temperatures below -20 °C.

Experimental Section

All kinetic experiments were carried out in resealable 5 mm NMR tubes fitted with a teflon valve purchased from Trillium Glass. H_2 was used as received (Air Products C. P., 99.3%), and acetone-d_6 (Aldrich Gold Label) was distilled from 4A molecular sieves. ^1H NMR spectra were recorded on a Bruker WH-400 spectrometer at 400.13 MHz. The temperature of the probe was regulated with a Bruker BVT-1000 temperature control unit.

The complex IrBr(CO)(dppe) was synthesized following the procedure previously reported.[6b]

General Procedure for Sample Preparation. A stock solution of IrBr(CO)(dppe) (9.55×10^{-3} M, 0.033 g of complex in 5 mL solvent) was prepared in acetone-d_6 and stored under N_2 in a dry box. For each experiment, 0.50 ± 0.02 mL of the stock solution was transferred to the NMR tube which was then connected to a high vacuum line containing an H_2 inlet. After three freeze-pump-thaw degas cycles, the solution was maintained at 0 °C in an ice bath while the sample was placed under the desired pressure of H_2 by opening the valve at the top of the NMR tube. The sample was then shaken thoroughly to ensure mixing of H_2, and placed in the thermostatted probe of the NMR spectrometer. The total volume of the NMR tube was determined to be 2.00 ± 0.05 mL with a solution volume for each run of 0.50 ± 0.05 mL.

RESULTS AND DISCUSSION

The kinetics of the isomerization reaction of the cis dihydrides of formula $IrH_2Br(CO)(dppe)$ has been studied over a wide range of H_2 pressures, from 12 mm to 670 mm of added H_2. The reactions were monitored by ^1H NMR

spectroscopy, using the integrals of the hydride resonances of isomers 3 and 4 to determine the relative amounts of each isomer present. Through comparison of the integral of the entire hydride region to the integral of the entire methylene region, the amount of unreacted IrBr(CO)(dppe) was determined. For each NMR tube experiment, 0.5 mL of a 9.55×10^{-3} M stock solution of IrBr(CO)(dppe), prepared and stored under nitrogen, was used.

Isomerization Under 670 mm of Hydrogen. The kinetic results of the isomerization of 3 to 4 under 670 mm of added H_2 reveal that the reaction proceeds by a clean first-order process. At 28 °C, the half-life for isomerization is 30 hours, and the corresponding k_{obs} is 3.85×10^{-4} min^{-1}. A plot of ln [3] vs. time is linear, as shown in Figure 1, essentially confirming the earlier results of Johnson and Eisenberg.[6a] As discussed in the Introduction, the isomerization mechanism favored by us previously was a reductive elimination/oxidative addition sequence shown as eqn (3) based on the fact that the initial oxidative addition was found to be fast and reversible. The rate law for this mechanism, given as eqn (4), depends only on the concentration of the kinetic dihydride 3, and shows no dependence on hydrogen pressure. Since the initial oxidative addition is highly stereoselective, k_{-1} is much greater than k_2 and the rate law (4) corresponds to that of a simple preequilibrium.

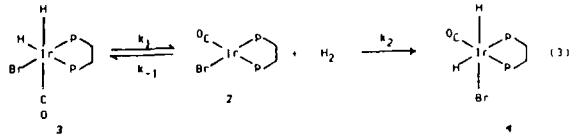

$$\frac{-d[3]}{dt} = k_{obs}[3] = \frac{k_1 k_2 [3]}{k_{-1} + k_2} - \frac{k_1 k_2 [3]}{k_{-1}} \qquad (4)$$

Isomerization under 200 to 450 mm of Hydrogen. The kinetics of isomerization for three experimental runs under 200, 300, and 450 mm of added H_2 were found to be approximately first order. That is, plots of ln [3] vs. time are linear for at least two half lives, although they show a slight deviation from linearity at early reaction times. This deviation is most evident at the lowest of these pressures of H_2 as shown in Figure 2. A more significant, and initially more puzzling, aspect of the kinetic runs under these pressures was that the rate of isomerization was observed to be faster as the pressure of added H_2 was lowered, as shown in Table 1. This variation in rate with H_2 pressure was inconsistent with the reductive elimination/-oxidative addition sequence of (3) and its rate law, (4), which shows no $[H_2]$ dependence. A plot of k_{obs} vs. $1/[H_2]$ suggested that a second isomerization pathway was operating in addition to (3), while showing that the inverse dependence of $[H_2]$ for this pathway was not strictly linear.

Isomerization Under Low Pressures of Hydrogen. Four experimental runs were carried out under 12, 22, 29, and 41 mm of added H_2, all of which correspond to amounts of added hydrogen less than one equivalent of starting complex, IrBr(CO)(dppe). These reactions proceeded much more quickly than those under higher pressures of H_2 - typically, isomerizations were complete in less than 15 hours. Attempts were made to fit the data to a first order equation, but plots of ln [3] vs. time showed significant deviations from linearity. Clearly, the isomerization path which was predominant at low pressures of H_2 did not follow first order kinetics.

A second order treatment of this experimental data was more successful in that plots of $1/[Ir_T]$ vs. time were linear, where Ir_T represents the sum of unreacted and unisomerized iridium complexes, 2 + 3. A plot of this data for the run under 22 mm of added H_2 is shown in Figure 3. Contrary to

expectations, the data in Table 2 show that the observed second order rate constant, k_{obs}, decreases with decreasing $[H_2]$, but a plot of k_{obs} vs. $[H_2]$ was found to be distinctly nonlinear. Surprisingly, a linear correlation was obtained when a plot of k_{obs} vs. $1/[H_2]$ was constructed as shown in Figure 4. The origin of this linear dependence on $1/[H_2]$ will become apparent below.

We thus conclude that an isomerization mechanism which is second order in complex predominates under low pressures of H_2 and possesses an inverse $[H_2]$ dependence.

Mechanism for the Second Order Isomerization Pathway. Under conditions in which less than one equivalent of H_2 is added to the reaction system, both IrBr(CO)(dppe) and the kinetic isomer of $IrH_2Br(CO)(dppe)$, 3, are present in observable concentrations. We propose a bimolecular mechanism involving these two species to explain the isomerization process under these conditions. This mechanism, which is consistent with the kinetic data, involves dihydride transfer between Ir species via a binuclear intermediate, 5, as shown in eqn (5).

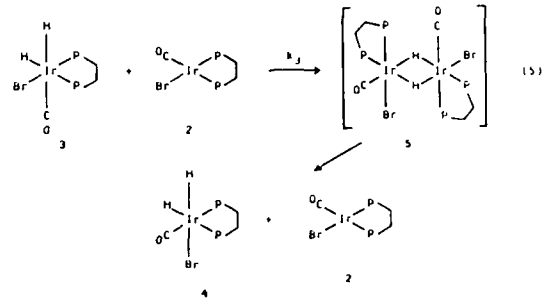

(5)

The proposal of a dihydride-bridged binuclear intermediate has precedents in other, closely related studies. In the investigation of the stereoselective oxidative addition of H_2 to various Ir(I) complexes of type 2, Johnson and Eisenberg described chemistry involving the reactive intermediate IrH(CO)(dppe) generated by dehydrohalogenation of $IrH_2Br(CO)(dppa)$, 4.[6a] When the reaction was carried out using the base DBU (1,8-diazabicyclo-[5.4.0]undec-7-ene) under H_2, the products were the trihydride $IrH_3(CO)(dppe)$, 6, and the kinetic dihydride 3, as shown in eqn (6). Use of D_2 showed that whereas most of 6 formed by the oxidative addition of H_2 (or D_2) to IrH(CO)(dppe), an amount roughly equivalent to the amount of 3-d_2 was produced via a different pathway. Since the thermodynamic dihydride 4 does not reductively eliminate H_2 on the time scale of the experiment, the formation of IrBr(CO)(dppe) which gives 3-d_2 upon reaction with D_2 was proposed to occur by direct dihydride transfer from $IrH_2Br(CO)(dppe)$ to IrH(CO)(dppe) through a bridged intermediate with concomitant formation of $IrH_3(CO)(dppe)$.

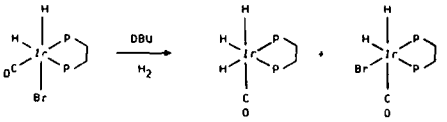

4 → 6 (85%) + 3 (15%) (6)

In an earlier report, Drouin and Harrod[8] proposed a dihydride-bridged dimer species in their attempts to convert the monodentate phosphine complex $IrH_3(CO)(P(p\text{-}ClC_6H_5)_3)_2$, 7, to the unsaturated complex $IrH(CO)(P(p\text{-}ClC_6H_5)_3)_2$, 8. When the trihydride 7 was placed under a stream of nitrogen to displace H_2, ^1H NMR evidence revealed the occurrence of an equilibrium proposed to

involve 9 as shown in eqn (7)

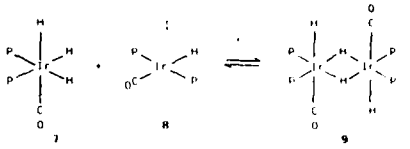

7 ⇌ 8 + H_2 ⇌ 9 (7)

Recently Jones and Maguire described the direct intermolecular transfer of H_2 between a rhenium complex and $IrBr(CO)(dppe)$.[9] Treatment of $(\eta^4\text{-}C_5H_6)Re(PPh_3)_2H_3$, 10, with 1 equivalent of IrBr(CO)(dppe), 2, resulted in the formation of $(\eta^5\text{-}C_5H_5)Re(PPh_3)_2H_2$ and the thermodynamic dihydride isomer of $IrH_2Br(CO)(dppe)$, 4, as shown in eqn (8). If the reaction had proceeded by elimination of H_2 from 10 followed by H_2 oxidative addition to 2, the kinetic isomer 3 would have been formed. A control experiment ruled out this possibility, and the results thus strongly support the notion that the reaction between 10 and 2 goes via a dihydride-bridged binuclear intermediate

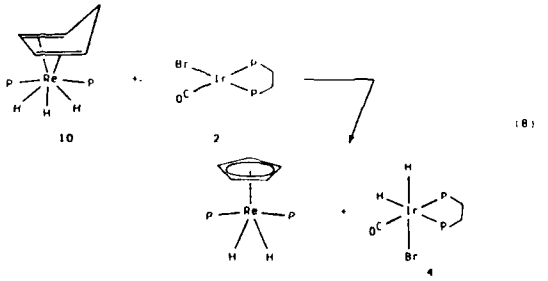

10 + 2 → F → Re(η⁵-C5H5)(PPh3)2H2 + 4 (8)

Rate Law for the Bimolecular Isomerization Pathway. The rate law for the

bimolecular isomerization mechanism shown above in eqn (5) is derived as follows beginning with (9).

$$\text{rate via bimolecular path} = k_3[3][2] \tag{9}$$

The concentrations of 2 and 3 are related by an equilibrium-constant expression where $[H_2]$ corresponds to the concentration of dissolved H_2. Therefore,

$$\frac{[3]}{[2][H_2]} = \frac{k_{-1}}{k_1} = K_{eq} \tag{10}$$

and

$$[3] = K_{eq}[2][H_2] \tag{11}$$

Substituting for [3] into eqn (9) yields (12):

$$\text{rate via bimolecular path} = k_3K_{eq}[2]^2[H_2] \tag{12}$$

We next express the rate in terms of $[Ir_T]$ corresponding to the sum of unreacted and unisomerized Ir species, [2] + [3]:

$$[Ir_T] = [2] + [3] = [2](1 + K_{eq}[H_2]) \tag{13}$$

$$[2] = \frac{[Ir_T]}{(1 + K_{eq}[H_2])} \tag{14}$$

Upon substitution of this expression for [2] into eqn (12) we obtain:

$$\text{rate via bimolecular path} = \frac{k_3K_{eq}\,[Ir_T]^2\,[H_2]}{(1 + K_{eq}[H_2])^2} \tag{15}$$

The $[H_2]$ dependence in rate expression (15) is complex, but it is evident that the value of $K_{eq}[H_2]$ determines the observed hydrogen dependence of the "second order" or bimolecular pathway. Two limiting regimes can be envisioned, which are as follows:

a) For $1 >> K_{eq}[H_2]$, the bimolecular rate = $k_3K_{eq}[Ir_T]^2[H_2]$. In this limit, the hydrogen concentration is extremely low, and the rate is proportional to $[H_2]$.

b) For $K_{eq}[H_2] >> 1$, the bimolecular rate = $k_3K_{eq}[Ir_T]^2/[H_2]$. When the hydrogen concentration is higher, the bimolecular rate becomes proportional to $1/[H_2]$.

The fact that the observed second order rate constant for isomerization shows an inverse $[H_2]$ dependence, as illustrated by the data in Table 2 and the plot in Figure 4, indicates that even at the low H_2 pressures used in the present isomerization study, $K_{eq}[H_2] >> 1$.

Isomerization Under an Intermediate Pressure of H_2. To examine the isomerization in between the high and low H_2 pressure regimes, an experiment was carried out under 120 mm of added H_2. Based on ^1H NMR integrations of the kinetic dihydride 3 and dissolved H_2, this initial pressure of H_2 corresponds to 1.03 equivalents of H_2 in solution. As in the high H_2 pressure regime, no IrBr(CO)(dppe) is observed in solution. The reaction is half complete in 3.5 hours, and surprisingly the best fit of the kinetic data is obtained when the reaction is treated as a second order, bimolecular process. That is, a reasonably straight line results from a plot of $1/[Ir_T]$ vs. time, Figure 5, where $[Ir_T]$ in this case represents the concentration of the kinetic dihydride 3.

The Complete Rate Law. The kinetic results described above indicate that both isomerization mechanisms operate to differing extents over the range of H_2 pressures examined. For a system with parallel reaction paths, the complete rate expression is given by the sum of the component rate laws. For the isomerization of $IrH_2Br(CO)(dppe)$, the complete rate expression is given by eqn (16) in which there are terms to account for both the first and second order components. If eqn (16) is correct, then it should be possible to fit the experimental data to this equation.

$$\text{(observed rate)}_{i} = \frac{k_2 [3]}{K_{eq}} + \frac{k_3 K_{eq} [Ir_T]^2 [H_2]}{1 + K_{eq}[H_2])^2} \qquad (16)$$

In order to do this, we analyze the kinetic data in terms of initial rate. Since this will give a rate value in M sec^{-1} for each run, unbiased by our perception of whether it is primarily in the first order or second order regime. In the initial rate limit, the value of $[Ir_T]$ corresponding to [2] + [3] is the same for each experiment (5.5×10^{-3} M), whereas the kinetic isomer concentration, [3], is measured throughout the course of each run. Initial rates for all kinetic runs were determined by fitting the experimental data ([3] vs. time) to a 5th order polynomial and extrapolating to t = 0. This allows us to ignore the concentration of the thermodynamic isomer 4. As seen in Table 3, the initial rate first increases with increasing $[H_2]$ and then turns over, decreasing as $[H_2]$ continues to increase. This is consistent with the functional dependence of $[H_2]$ in eqn (15) and its two limiting cases described above.

The concentration of H_2 in solution, $[H_2]$, for each experiment is calculated using the material balance expression, eqn (17), where $P_o(H_2)$ is the initial added pressure of H_2 in atmospheres, V_{gas} is the volume above the solution in the NMR tube (1.5 ± 0.05 mL), and V_{sol} is the solution volume (0.5 mL).

$$\frac{P_o(H_2) V_{gas}}{RT} = \frac{P(H_2) V_{gas}}{RT} + [H_2] V_{sol} + [3] V_{sol} \qquad (17)$$

The total amount of added hydrogen, $P_o(H_2)V_{gas}/RT$, is distributed as the amount in solution, $[H_2]V_{sol}$, the amount above the solution, $P(H_2)V_{gas}/RT$, and the amount which is consumed to make dihydride, $[3]V_{sol}$. Substitutions are made for $P(H_2)$ using a modified form of Henry's Law (i.e., $P(H_2) = [H_2]/K_h$), and for [3] (recalling the equilibrium of eqn (1)).

$$\frac{P_o(H_2) V_{gas}}{RT} = \frac{[H_2] V_{gas}}{RTK_h} + [H_2] V_{sol} + K_{eq}[2][H_2] V_{sol} \qquad (18)$$

Substituting $[Ir_T]$-[3] for [2] in (18) and solving for $[H_2]$ leads to

$$[H_2] = \frac{P_o(H_2) V_{gas} / RT}{(V_{gas}/RTK_h) + V_{sol} + V_{sol} K_{eq}([Ir_T] - [3])} \qquad (19)$$

Values for $P_o(H_2)$ are known for each experiment, and a value for Henry's constant, K_h, was determined experimentally to be 3.16×10^{-3} M/atm by measuring $[H_2]$ in acetone-d_6 using ^1H NMR spectroscopy as a function of $P_o(H_2)$. Thus the concentration of hydrogen in solution is determined for each kinetic run.

A slight rearrangement of eqn (16) yields an expression for a "reduced rate", eqn (20), equivalent to subtracting out the contribution of the first order component from the observed initial rate:

$$\text{reduced rate} = \text{observed initial rate} - \frac{k_2 [3]}{K_{eq}} = \frac{k_3 K_{eq} [Ir_T]^2 [H_2]}{(1 + K_{eq}[H_2])^2} \qquad (20)$$

A plot of reduced rate vs $([H_2]/(1 + K_{eq}[H_2])^2)$ should give a straight line with a slope = $k_3 K_{eq} [Ir_T]^2$. As shown in figure 6, the experimental data fit the derived function reasonably well with two clusters of data points corresponding to the two pressure regimes studied, one with more than 1 equivalent of added H_2 and the other with less than 1 equivalent. The fit of the line indicates that the derived equation accurately describes the behavior of the system. The data which are plotted, as well as values for $P_o(H_2)$, [3], and $[H_2]$, are given in Table 3.

The very small values for the reduced rate at high $[H_2]$ indicate little contribution from the second order pathway. From runs at the highest added H_2 pressure, we estimate that k_{obs} is approximately k_2/K_{eq} and has a value of 3 ×

$\times 10^{-4}$ min^{-1}. Different values of the equilibrium constant, K_{eq}, were employed in plotting the data with the best trial and-error fit obtained using 2.8 $\times$ 10^{-4} M^{-1}. Based on this value and the fact that the slope of the line in Fig. 6 is $k_3 K_{eq}[(r_1)]^2$, we estimate the bimolecular rate constant for isomerization, k_3, to be 0.21 M^{-1} min^{-1}.

Low Temperature Evidence of the Bimolecular Pathway. Further confirmation of the bimolecular mechanism for isomerization was demonstrated by a low temperature experiment which showed that in the H_2 deficient regime isomerization of $IrH_2(CO)(dppe)$ can occur even when the reductive elimination/oxidative addition path is completely shut down. In one NMR tube, a sample of the kinetic dihydride 3 was prepared by addition of 500 mm of H_2 to IrBr(CO)(dppe), and kept below -50 °C to prevent it from isomerizing. The excess H_2 was removed by two *freeze-pump-thaw cycles, and 200 mm* of D_2 were added. After shaking the sample to ensure mixing of D_2, the tube was maintained at -23 °C for 24 hours. A ^{1}H NMR spectrum taken at -23 °C showed no isomerization to 4, and no incorporation of D_2 into 3 by integration of the hydride resonances relative to the methylene resonances. This confirmed that reductive elimination of H_2 from $IrH_2(CO)(dppe)$ does not occur at -23 °C over a 24 hour period. A second NMR sample was prepared by adding 25 mm of H_2 (< 1 equivalent) to IrBr(CO)(dppe). After maintaining this sample at -23 °C for 24 hours, a ^{1}H NMR spectrum revealed that isomerization had occurred to the extent of 31%. This experiment thus confirmed that isomerization of 3 to 4 can occur independent of the reductive elimination of hydrogen from $IrH_2Br(CO)(dppe)$ by a bimolecular path.

Stereoselectivity of Dihydride Transfer. In light of the stereoselective oxidative addition of H_2 to IrBr(CO)(dppe) to give the kinetic isomer 3, it is interesting to consider why the dihydride transfer produces the thermodynamic isomer 4. That is, *why does dihydride transfer to 2 proceed with opposite* stereoselectivity to that of H_2 oxidative addition? The answer must be electronic in nature since steric factors for the formation of the two isomers of $IrH_2Br(CO)(dppe)$ by dihydride transfer are similar.

In H_2 oxidative addition, there are two principal interactions between the d^8 metal complex and the H_2 molecule.[10] The first involves a donation from the $\sigma^b(H_2)$ orbital into a vacant acceptor orbital on the metal center of p_z or p_z-d_{z^2} hybrid character, while the second is a back-bonding interaction in which electron density is transferred from a filled metal d_π orbital into the σ^* orbital of H_2. In addition to this synergic interaction, a repulsive 4-e$^-$ interaction between the filled $\sigma^b(H_2)$ and d_{z^2} orbitals has been invoked as a major contributor to the activation barrier in the H_2 oxidative addition process.[10c]

The stereoselectivity of H_2 oxidative addition to 2 arises by a preferred bending of one set of trans ligands in 2 which become cis to each other and trans to the hydride ligands in the product, as shown in A. This preference relates to the 4-e$^-$ repulsive interaction between $\sigma^b(H_2)$ and d_{z^2}. As H_2 approaches the metal complex, one pair of trans ligands bends such that complex + substrate form a trigonal bipyramid as the transition state with the bending ligands and H_2 occupying the TBP equatorial positions. Preference for bending of the P-Ir-CO axis over the P-Ir-X axis in 2 (i.e., preference for A over B) occurs because this places the better π-acid ligand, CO, in the equatorial plane where it can better stabilize the developing trigonal bipyramid through backbonding and withdrawal of electron density from d_{z^2}, thereby reducing the repulsive interaction.

In dihydride transfer, the interaction between the square planar Ir(I) complex and the MH_2 substrate is *not a synergic one.* If one considers MH_2 to approach the d^8 complex in a symmetrical manner with equal Ir---H distances, there is no substrate orbital which corresponds to $\sigma^b(H_2)$. Hence, the 4-e$^-$

repulsive interaction does not exist, and the principal reason for addition along the P-Ir-CO axis is removed. In fact, the better d_π donor orbital in IrBr(CO)(dppe) is the one oriented in the plane defined by P-Ir-Br and the z axis, and it is in this plane that dihydride transfer occurs. While a detailed theoretical analysis of dihydride transfer remains to be done, we envision that the major orbital interaction takes place between a filled d_π orbital of Ir(I) and the σ^* function of MH_2 possessing the same symmetry.

Conclusions

The kinetic studies which we have described involving the isomerization of the dihydrides of $IrH_2Br(CO)(dppe)$ show that the reaction proceeds via two different mechanisms. Both mechanisms operate to differing extents throughout the range of H_2 concentrations examined, but two limiting regimes may be defined as greater than and less than one equivalent of H_2 relative to the unsaturated starting complex, IrBr(CO)(dppe).

In the presence of excess added hydrogen, the isomerization of 3 to 4 occurs primarily by the first-order reductive elimination/H_2 oxidative addition sequence shown in eqn (3). The rate law for this mechanism shows no dependence on $[H_2]$. However, the half-life for isomerization in this regime ($P_o(H_2)$ > 200 mm) decreases with decreasing $[H_2]$, indicating that the other mechanism which is H_2 dependent also operates under these conditions.

The reaction path which predominates under hydrogen deficient conditions involves direct dihydride transfer through a binuclear hydride- bridged species. This pathway is dependent on $[H_2]$, is second order with respect to complex, and follows the rate law shown in eqn (15).

Through the use of initial rates, the kinetic data have been accommodated into a single rate expression having first and second order components. The fit of the data to eqn (20) yields an experimental value for the second-order dihydride transfer rate constant, k_{H_2} = [illegible] M^{-1} min^{-1}.

One of the most significant aspects of the study of the species IrBr(CO)(d_2-dppe)(H_2) is the ease with which D_2 effectively from a metal polyhydride complex by dihydride the formation of stable binuclear hydride bridged complexes in which unusual feature about the present study is that the transfer of H_2 metal center to the other is complete under mild conditions. of H_2 from polyhydride complexes to achieve coordinative unsaturation requires forcing thermal or photochemical conditions, we think that an alternative approach based on the H_2 abstracting ability of 2 might be attractive. If, indeed, complex 2 does abstract H_2 from other polyhydride substrates L_nMH_x, then dihydride transfer may become an effective method for preparing highly reactive, coordinatively unsaturated species, L_nMH_{x-2}, for C-H bond activation studies. This approach is presently under investigation.

Acknowledgements. We wish to thank the National Science Foundation (CHE 83-08064) and the Office of Naval Research for support of this work, and Johnson Matthey Co., Inc. for a generous loan of iridium salts. We also wish to thank Mr. Ramy Farid for assistance with the figures.

REFERENCES AND FOOTNOTES

1. Collman, J. P.; Hegedus, L. S.; Norton, J. R.; Finke, R. G. "Principles and Applications of Organotransition Metal Chemistry", University Science Books, Mill Valley, CA, 1980, Chap. 6. Cotton, F. A.; Wilkinson, G. "Advanced Inorganic Chemistry", 4th Ed., Wiley, Interscience, New York, 1980, Chapter 30.
2. Marshall, J. W. "Homogeneous Catalysis", Wiley/Interscience, New York, NY, 1980, Chapters 3 and 5 and references therein. Atwood, J. D. "Inorganic and Organometallic Reaction Mechanisms", Brooks/Cole Publishing, Monterey, CA, 1985, Chap. 5 and references therein.
3. Vaska, L. Acc. Chem. Res. 1968, 1, 335.
4. (a) Chock, P. B.; Halpern, J. J. Am. Chem. Soc. 1966, 88, 3511. (b) Vaska, L.; Werneke, M. F. Trans. N. Y. Acad. Sci. 1971, 33, 70. (c) Ugo, R.; Pasini, A.; Fusi, A.; Cenini, S. J. Am. Chem. Soc. 1972, 94, 7364. (d) Strohmeier, W.; Onada, T. Z. Naturforsch. 1968, 23b, 1527. (e) Strohmeier, W.; Muller, F. J. Z. Naturforsch. 1969, 24b, 931. (f) Deeming, A. J.; Shaw, B. L. J. Chem. Soc. (A) 1966, 1128.
5. Two reviews cite the pertinent literature in addition to those given in reference 4. (a) James, B. R. "Homogeneous Hydrogenation", Wiley, New York, 1973, Chapter 12. (b) James, B. R. In "Comprehensive Organometallic Chemistry", Wilkinson, G.; Stone, F. G. A.; Abel, E. W., Eds., Pergamon Press, New York, 1982, Vol. 8, Chapter 51.
6. (a) Johnson, C. E.; Eisenberg, R. J. Am. Chem. Soc. 1985, 107, 3148. (b) Johnson, C. E.; Fisher, B. J.; Eisenberg, R. J. Am. Chem. Soc. 1983, 105, 7772.
Johnson, C. E.; Eisenberg, R. J. Am. Chem. Soc. 1985, 107, 6531.
9. Jones, W. D.; Maguire, J. A. J. Am. Chem. Soc. 1985, 107, 4544.
10. (a) Saillard, J. Y.; Hoffmann, R. J. Am. Chem. Soc. 1984, 106, 2006. (b) Sevin, A. Nouv. J. Chim. 1981, 5, 233. (c) Dedieu, A.; Strich, A. Inorg. Chem. 1979, 18, 2940. (d) Noell, J. O.; Hay, P. J. J. Am. Chem. Soc. 1982, 104, 4578.
11. Venanzi, L. M. Coord. Chem. Rev. 1982, 43, 251.

TABLE 1

Kinetic Data for the Isomerization of 3 to 4 under High H_2 Pressure

H_2, mm	Total Equiv of Added H_2[a]	Equiv of H_2 in Soln[b]	First Order Rate Constant ($\times 10^4$), min^{-1}
200	3.36	1.07	6.73
300	5.03	1.11	4.64
450	7.55	1.18	4.32
670	11.24	1.22	1.85

[a] Calculated from $P_0(H_2) V_{gas} / RT(9.55 \times 10^{-3}) MV_{sol}$ where V_{gas} and V_{sol} are the volumes of the gas and solution phases, respectively, of the NMR tube and 9.55×10^{-3} M is the concentration of the starting iridium complex in solution.

[b] Based on the measured concentrations of H_2, 3 and total dppe species as described in the text. The value shown is given by the expression $([H_2] + [3]) / ([2] + [3]) - ([H_2] + [3])/[3]$

TABLE 2

Kinetic Data for the Isomerization of 3 to 4 Under Low H_2 Pressure

H_2, mm	Initial ratio of $[3]/[Ir_T]$[a]	Second Order Rate Constant, M^{-1} min^{-1}
12	0.43	0.211
22	0.61	0.398
29	0.76	0.445
41	0.92	0.494

[a] Based on the measured concentrations of 3 and total dppe species as described in the text.

TABLE 3

Initial Rate Data for the Isomerization of 3 to 4 for All H_2 Pressures

$p_{(H_2)}$, mm	$[H_2]_{soln}$ ($\times 10^5$), M	$\frac{[H_2]}{1 + K_{eq}[H_2]}$ ($\times 10^7$), M	[3] ($\times 10^3$), M	Initial rate ($\times 10^6$), M min^{-1}	Reduced rate ($\times 10^7$), M min^{-1}
12	1.02	81.1	4.10	25.2	238.0
22	2.47	86.2	5.83	35.9	340.0
29	4.49	88.1	7.26	32.2	298.0
41	11.1	86.6	8.79	28.5	256.0
120	48.9	22.7	9.55	10.8	76.5
200	81.5	14.4	9.55	8.63	54.8
300	122.0	9.87	9.55	5.77	26.2
450	183.0	6.70	9.55	3.97	8.18
670	272.0	4.56	9.55	3.69	5.38

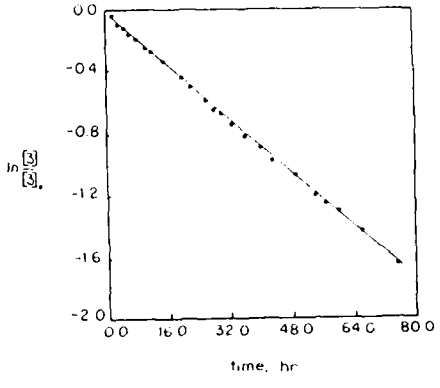

Figure 1. First order plot for the isomerization of $IrH_2Br(CO)(dppe)$ under 670 mm of added H_2.

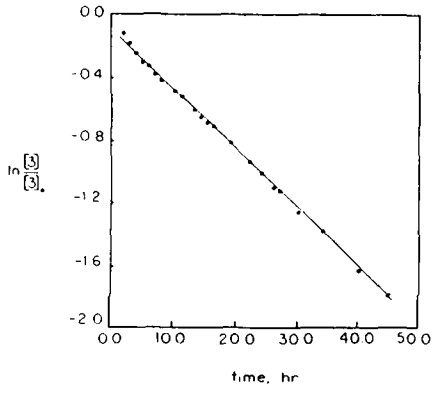

Figure 2. First order plot for the isomerization of $IrH_2Br(CO)(dppe)$ under 200 mm of added H_2.

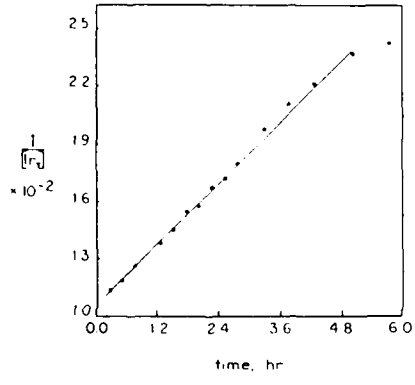

Figure 3. Second order plot, $1/[Ir_T]$ vs. time, for the isomerization of $IrH_2Br(CO)(dppe)$ under 22 mm of added H_2.

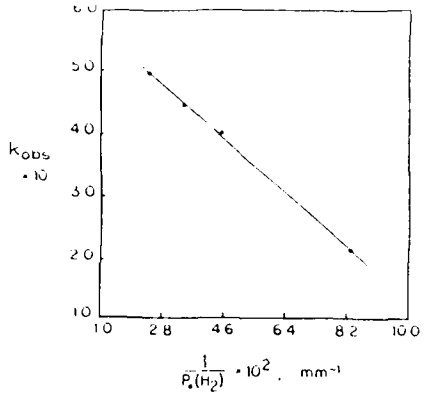

Figure 4. Plot of the observed second order rate constants, k_{obs} vs $1/P_e(H_2)$ for the isomerization of $IrH_2Br(CO)(dppe)$ with less than one equivalent of added H_2.

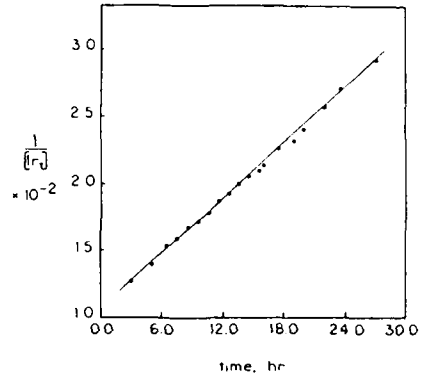

Figure 5. Second order plot, $1/([Ir_1])$ vs time, for the isomerization of $IrH_2Br(CO)(dppe)$ under 120 mm of added H_2.

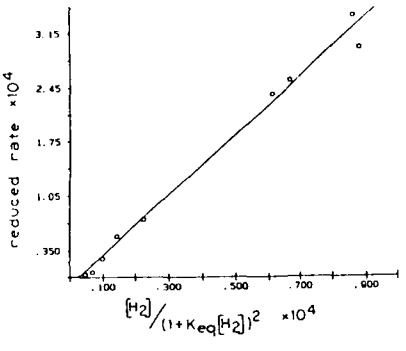

Figure 6. Plot of the reduced rate defined in eqn (20) vs the function describing the $[H_2]$ dependence in the complete rate law.

TECHNICAL REPORT DISTRIBUTION LIST, GEN

	No. Copies
Office of Naval Research Attn: Code 1113 800 N. Quincy Street Arlington, Virginia 22217-5000	2
Dr. Bernard Douda Naval Weapons Support Center Code 50C Crane, Indiana 47522-5050	1
Naval Civil Engineering Laboratory Attn: Dr. R. W. Drisko, Code L52 Port Hueneme, California 93401	1
Defense Technical Information Center Building 5, Cameron Station Alexandria, Virginia 22314	12 high quality
DTNSROC Attn: Dr. H. Singerman Applied Chemistry Division Annapolis, Maryland 21401	1
Dr. William Tolles Superintendent Chemistry Division, Code 6100 Naval Research Laboratory Washington, D.C. 20375-5000	1
Dr. David Young Code 334 NORDA NSTL, Mississippi 39529	1
Naval Weapons Center Attn: Dr. Ron Atkins Chemistry Division China Lake, California 93555	1
Scientific Advisor Commandant of the Marine Corps Code RD-1 Washington, D.C. 20380	1
U.S. Army Research Office Attn: CRD-AA-IP P.O. Box 12211 Research Triangle Park, NC 27709	1
Mr. John Boyle Materials Branch Naval Ship Engineering Center Philadelphia, Pennsylvania 19112	1
Naval Ocean Systems Center Attn: Dr. S. Yamamoto Marine Sciences Division San Diego, California 92132	1

END

DATE
FILMED

1-87

DTIC